Domains on the hepatitis C virus internal ribosome entry site for 40s subunit binding

J. ROBIN LYTLE,[1,2] LILY WU,[1] and HUGH D. ROBERTSON[1]

[1]Department of Biochemistry, Weill Medical College of Cornell University, New York, New York 10021, USA

ABSTRACT

The internal ribosome entry site (IRES) of the hepatitis C virus (HCV) RNA is known to interact with the 40S ribosomal subunit alone, in the absence of any additional initiation factors or Met-tRNA$_i$. Previous work from this laboratory on the 80S and 48S ribosomal initiation complexes involving the HCV IRES showed that stem-loop III, the pseudoknot domain, and some coding sequence were protected from pancreatic RNase digestion. Stem-loop II is never protected by these complexes. Furthermore, there is no prior evidence reported showing extensive direct binding of stem-loop II to ribosomes or subunits. Using direct analysis of RNase-protected HCV IRES domains bound to 40S ribosomal subunits, we have determined that stem-loops II and III and the pseudoknot of the HCV IRES are involved in this initial binding step. The start AUG codon is only minimally protected. The HCV-40S subunit binary complex thus involves recognition and binding of stem-loop II, revealing its role in the first step of a multistep initiation process that may also involve rearrangement of the bound IRES RNA as it progresses.

Keywords: 40S subunit; hepatitis C virus; internal ribosome entry site (IRES); RNase protection; translation initiation

INTRODUCTION

Eukaryotic protein synthesis begins with the assembly of several initiation factors, Met-tRNA$_i$, and GTP on the 40S small ribosomal subunit. The 40S ribosomal subunit can only associate with capped, eukaryotic mRNA after first binding the initiator tRNA. The initial contact between the mRNA and the 40S subunit forms through a protein–protein bridge involving eIF4G and eIF3 (Dever, 1999; Hershey & Merrick, 2000; Pestova et al., 2001). The hepatitis C virus (HCV) mRNA, on the other hand, can not only bypass the eukaryotic need for a capped 5′ end, but, like prokaryotic mRNA, it can bind to the 40S subunit before Met-tRNA$_i$ (Pestova et al., 1998). Deletion of the initiation codon and coding region, which lie within the internal ribosome entry site (IRES) boundaries, did not prevent 40S subunits from binding to the HCV IRES. These investigators also used primer extension inhibition to determine indirectly that the 3′ border of the HCV IRES bound to the 40S subunit is in stem-loop IV (Fig. 1).

The HCV mRNA's factor-independent ability to bind to the small subunit is unique for eukaryotic cellular and viral mRNAs. Using ribosomes or subunits to protect key regions of mRNA from RNase digestion, we previously studied translation inhibitor-induced 48S and 80S ribosomal complexes with the HCV IRES (Lytle et al., 2001). Here we report similar experiments on the simpler preinitiation complex between the HCV IRES and salt-washed 40S ribosomal subunits. Several recent studies (Kolupaeva et al., 2000; Kieft et al., 2001; Spahn et al., 2001) have illustrated that the 40S subunit can interact specifically with the HCV IRES in the absence of any other macromolecular components. It has not been shown whether this binary complex is a true translation intermediate in vivo. Nonetheless, work by Kieft et al. (2001), which showed that the presence or absence of factor eIF3 has little effect on the binding affinity of 40S subunits to the HCV IRES, supports the idea that identifying the HCV IRES domains involved in the binary complex will help to elucidate the initial steps of HCV translation.

Nearly all of the HCV 5′ untranslated region (5′ UTR) and some coding sequence are necessary for protein synthesis. Residues 40 through 372 are required for full translational activity (Fukushi et al., 1994; Rijnbrand et al., 1995; Honda et al., 1996; Reynolds et al., 1996). Some of these studies suggest a need for stem-loop II
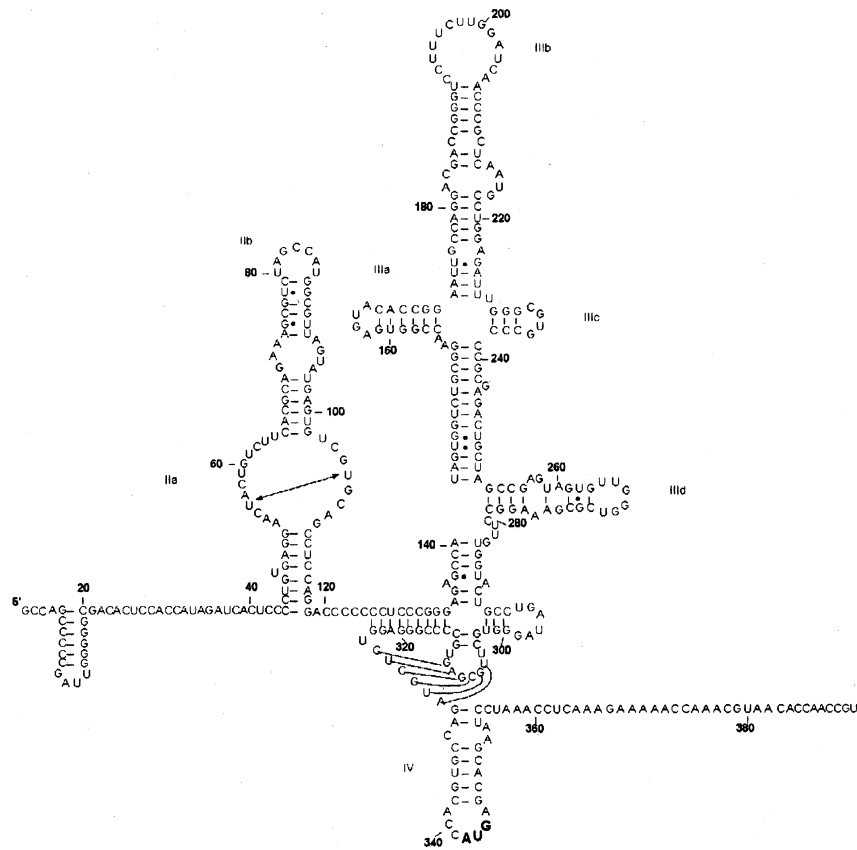
FIGURE 1. A UV-crosslinkable tertiary element in HCV IRES RNA. A UV crosslink was identified between bases U56 and U106, suggesting that an element of local tertiary structure resides in the lower portion of stem-loop II (Lyons et al., 2001).

sequences for translation, but no direct role for them in ribosome binding. Work we have published previously identifying the domains of the HCV IRES that interact with the 80S and the 48S ribosomal complexes (Lytle et al., 2001) point to a similar conclusion. Stem-loops III and the pseudoknot were protected by both ribosomal complexes. The 48S ribosomal complex protects half of stem-loop IV, the start AUG codon and 13 bases of coding sequence. The 80S ribosomal complex interacts with stem-loop IV, the start codon, and 50 bases of coding sequence. However, even though stem-loop II is necessary for HCV protein synthesis, it is not protected in either of these ribosomal complexes.

Stem-loop II, which lies between residues 44 and 118 of the HCV IRES, is considered to be its 5′ boundary (Fukushi et al., 1994; Rijnbrand et al., 1995; Honda et al., 1996, 1999; Reynolds et al., 1996). Domains spanning residues 28–69, 70–97, and 5–104 are essential for HCV IRES function in vitro and in vivo (Rijnbrand et al., 1995). Deletion of nt 103 to 114 leads to negligible IRES activity and residues 47 through 67 are essential for the IRES to initiate translation (Fukushi et al., 1994). Similarly, residues 23 through 102 are necessary for protein synthesis (Odreman-Macchioli et al., 2000).

Previously published work from this laboratory has identified a preexisting element of local tertiary struc-

ture involving bases U56 and U106 and their surrounding sequences in stem-loop II of the HCV IRES (Fig. 1; Lyons et al., 2001). As has been observed many times in the past (Branch et al., 1985; Romaniuk, 1989; Allison et al., 1991; Wimberly et al., 1993), such UV-crosslinkable tertiary elements as that in stem-loop II may be sites of protein binding. In fact, a 25-kDa protein, later identified as protein S5 from the 40S subunit, was shown to crosslink through a bridging linker to the HCV IRES in a way that somehow depended on stem-loop II sequences (Pestova et al., 1998; Fukushi et al., 1999, 2001; Odreman-Macchioli et al., 2001). It has recently been suggested that the actual binding site for protein S5 is in stem-loop III (Kolupaeva et al., 2000; Pestova et al., 2001), thus removing any need for direct ribosome–stem-loop II interaction.

With regard to IRES-containing mRNAs, so far only indirect studies of 40S preinitiation complexes using HCV IRES mRNA sequences have been reported. These experiments employed toeprinting assays that detect blocks to primer extension after various treatments of the IRES RNA (Pestova et al., 1998; Kolupaeva et al., 2000), or footprinting of end-labeled IRES RNA after partial cleavage by enzymes or chemicals (Kieft et al., 2001). These assays generally only give information about the downstream edge of the ribosomal-HCV RNA contact; or about unpaired resi-

dues that can be attacked by the chemical agents employed.

As in our previous report on HCV 48S and 80S initiation complexes (Lytle et al., 2001), we have studied the HCV IRES–40S ribosomal subunit complex by a "bind and chew" method, in which the fragments of internally labeled mRNA that are protected from exhaustive RNase digestion are recovered, their sequences determined and their positions mapped. The pancreatic RNase enzyme used for our studies has a considerably larger molecular size than the chemical reagents (e.g., dimethyl sulphate and diethyl pyrocarbonate) used for footprinting. It is therefore likely that any sequences detected by footprinting must lie in intimate contact with the ribosomal surface, whereas those identified by our enzymatic approach must lie in close proximity to the ribosome, but not necessarily in intimate contact with it. Our approach using generally labeled HCV IRES RNA, because it does not favor downstream versus upstream or base-paired versus single-stranded sequences, may give a more balanced result.

To determine directly whether stem-loop II is involved in 40S subunit interaction, we have identified those parts of the HCV IRES that interact with the 40S ribosomal subunit in preinitiation binary complexes using pancreatic RNase protection. We find that extensive sequences from both stem-loop II and stem-loop III are involved in this first step of HCV IRES-directed protein synthesis initiation, suggesting a multistep pathway during which structural rearrangement of the IRES takes place.

RESULTS

Internally labeled transcripts containing the complete HCV 5′ UTR and various lengths of HCV mRNA coding sequence were incubated with purified, salt-washed 40S ribosomal subunits (Fig. 2). Capped eukaryotic β-globin mRNA was used as a control. The HCV mRNA formed a complex that could withstand sucrose density gradient centrifugation. This complex could also withstand RNase treatment (Fig. 2A). As expected, β-globin mRNA does not bind to salt-washed 40S subunits without bridging initiation factors or Met-tRNA$_i$ (Fig. 2B). Furthermore, the HCV-40S complex cannot form in the presence of EDTA (Fig. 3B). In addition, the HCV IRES cannot independently bind to salt-washed 60S subunits, unlike 40S subunits (Fig. 3C).

Following RNase digestion and sucrose gradient centrifugation (Fig. 2A), the fractions from the gradient containing the HCV-40S complex peak were pooled. The protected radiolabeled RNA fragments from the HCV-40S complex were isolated and electrophoresed on a denaturing, polyacrylamide gel (Fig. 4, lane 3). The protected gel band pattern of the HCV-40S complex is distinct from the band patterns of anisomycin-induced 80S and edeine-induced 48S ribosomal complexes,
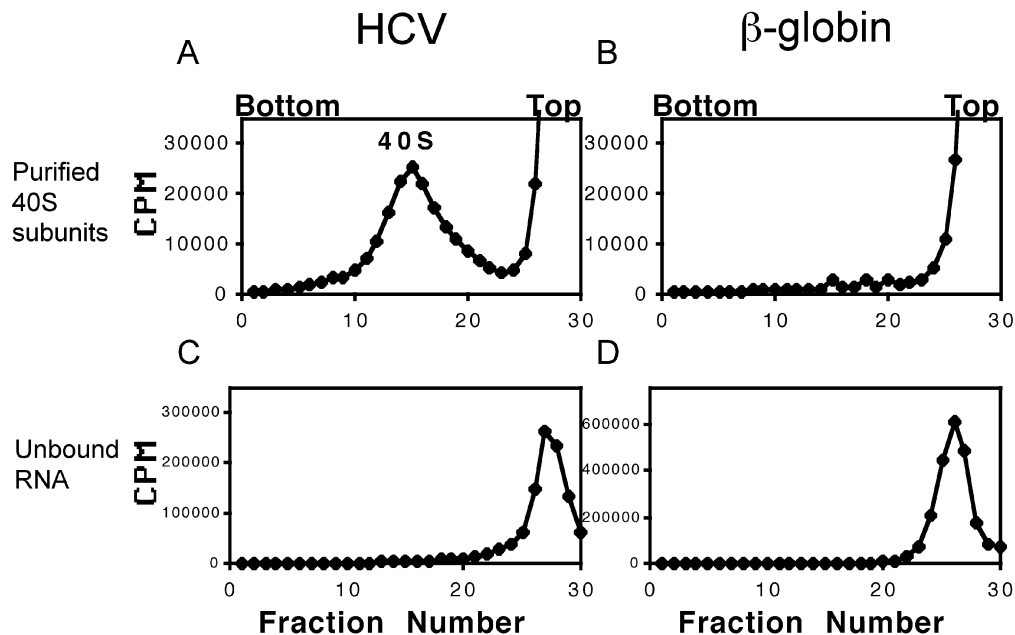

FIGURE 2. Sedimentation profile of the HCV IRES and purified 40S subunits. **A, B:** Sucrose gradient sedimentation profiles of radiolabeled 645-base HCV or 602-base β-globin RNAs incubated with salt-washed 40S ribosomal subunits, treated with RNase, and centrifuged in sucrose density gradients containing 1 mM MgCl$_2$. **C, D:** Sedimentation profiles of radiolabeled HCV or β-globin RNAs incubated in buffer and centrifuged on sucrose density gradients containing 1 mM MgCl$_2$. Both the HCV and β-globin RNAs are of approximately equal lengths of about 600 bases. All profiles show the counts per minute plotted against the fraction number of the gradient. The first fraction is taken from the bottom of the gradient and the last from the top. The 40S ribosomal peak is indicated.
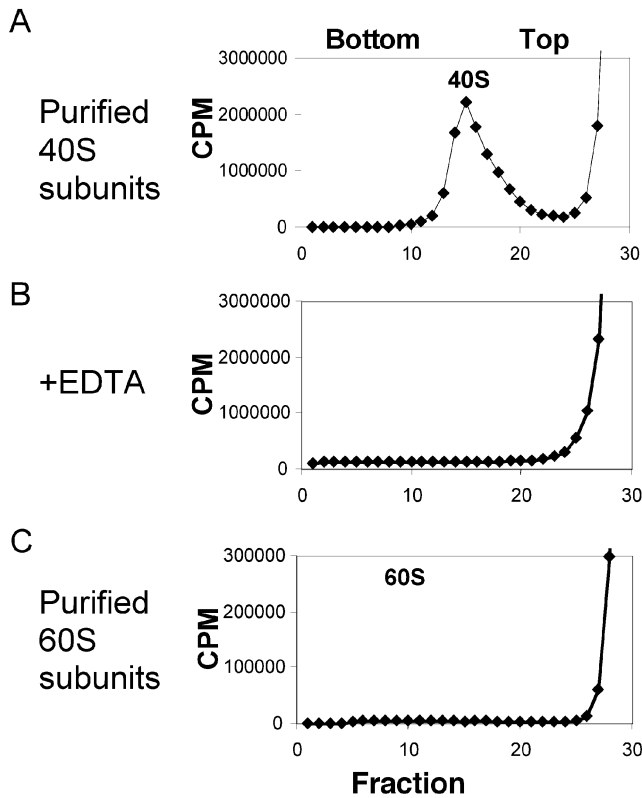
A

Purified
40S
subunits

B

+EDTA

C

Purified
60S
subunits

FIGURE 3. Sedimentation profiles of HCV RNA with 40S and 60S subunits. **A:** Sucrose gradient sedimentation profile of radiolabeled 645-base HCV RNA incubated with salt-washed 40S ribosomal subunits, treated with RNase, and centrifuged. **B:** Sedimentation profile of radiolabeled HCV RNA incubated with purified 40S subunits and 10 mM EDTA, treated with RNase, and centrifuged. **C:** Sedimentation profile of radiolabeled HCV RNA incubated with purified 60S subunits, treated with RNase, and centrifuged. All profiles show the counts per minute plotted against the fraction number of the gradient. The first fraction is taken from the bottom of the gradient and the last from the top. The 40S ribosomal peak and the missing 60S peak are indicated.

FIGURE 4. Polyacrylamide gel analysis of RNA fragments of the 40S subunit protection pattern compared to those of 80S and 48S ribosomal complexes. The HCV protected RNA fragments from 80S (lane 1) and 48S (lane 2) complexes and 40S ribosomal subunits (lane 3) were electrophoresed on a denaturing, 15% polyacrylamide gel. The 80S and 48S protected fragments have similar band patterns, whereas the band pattern of the 40S subunit is different. Two prominent bands of HCV RNA protected by purified 40S subunits are marked as a and b. O: origin; XC: xylene cyanol; Bϕ, bromophenol blue.

which were both very similar to each other (Fig. 4, lanes 1 and 2). However, like the protected bands from the 80S and 48S ribosomal complexes, which were examined in our previous publication (Lytle et al., 2001), the 40S-protected RNA fragments range in size from over 100 bases to 10 bases in length.

The majority of the bands were extracted from the gel and subjected to RNA fingerprinting. The resulting RNase T1-resistant oligomers were then digested in further RNase secondary analyses. Many of the recovered 40S-protected RNA fragments were similar to those found in both the 80S and 48S ribosomal complexes previously studied (Lytle et al., 2001). However, two prominent bands in particular contained sequences not protected by either of the 80S or 48S ribosomal complexes (Fig. 5A). Band a was isolated and subjected to RNA fingerprinting (Fig. 5B). Each of the RNase T1-resistant oligomers in the RNA fingerprint was extracted and separate aliquots were treated with pan-
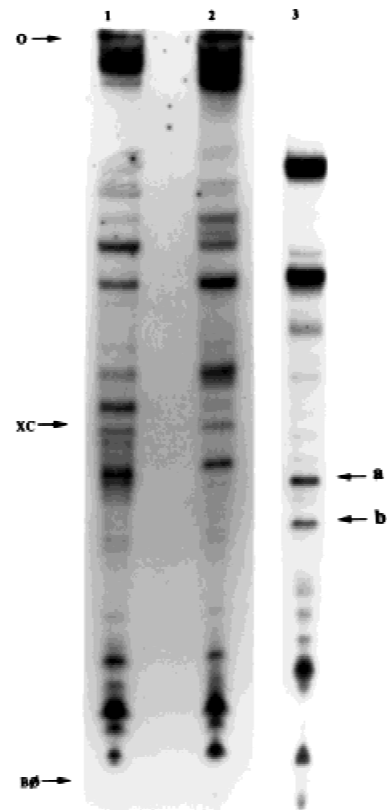
creatic RNase and alkaline hydrolysis. The oligomers' mobility on the fingerprint and their digestion products were used to determine the sequence of the fragment, which is listed beside each oligomer in Figure 5B. Band a contains a fragment spanning bases 85–111. Band b contains bases 57–78. Band b co-ran with a second sequence in the polyacrylamide gel. The oligomers from this separate sequence are labeled spots X and Y in Figure 5B. Each of the protected fragments a and b is depicted on the secondary structure map in Figure 5C. Band b lies on the left side of stem-loop II, whereas band a lies on the right side.

Each of the fragments from the experiment in lane 3 of the gel in Figure 4 and the bands from three other independent trials were isolated and fingerprinted. The RNase T1-resistant oligomers from the fingerprints were subjected to further RNase analyses. The sequence of each of the 40S protected HCV fragments was determined. All of the recovered fragments lie between bases
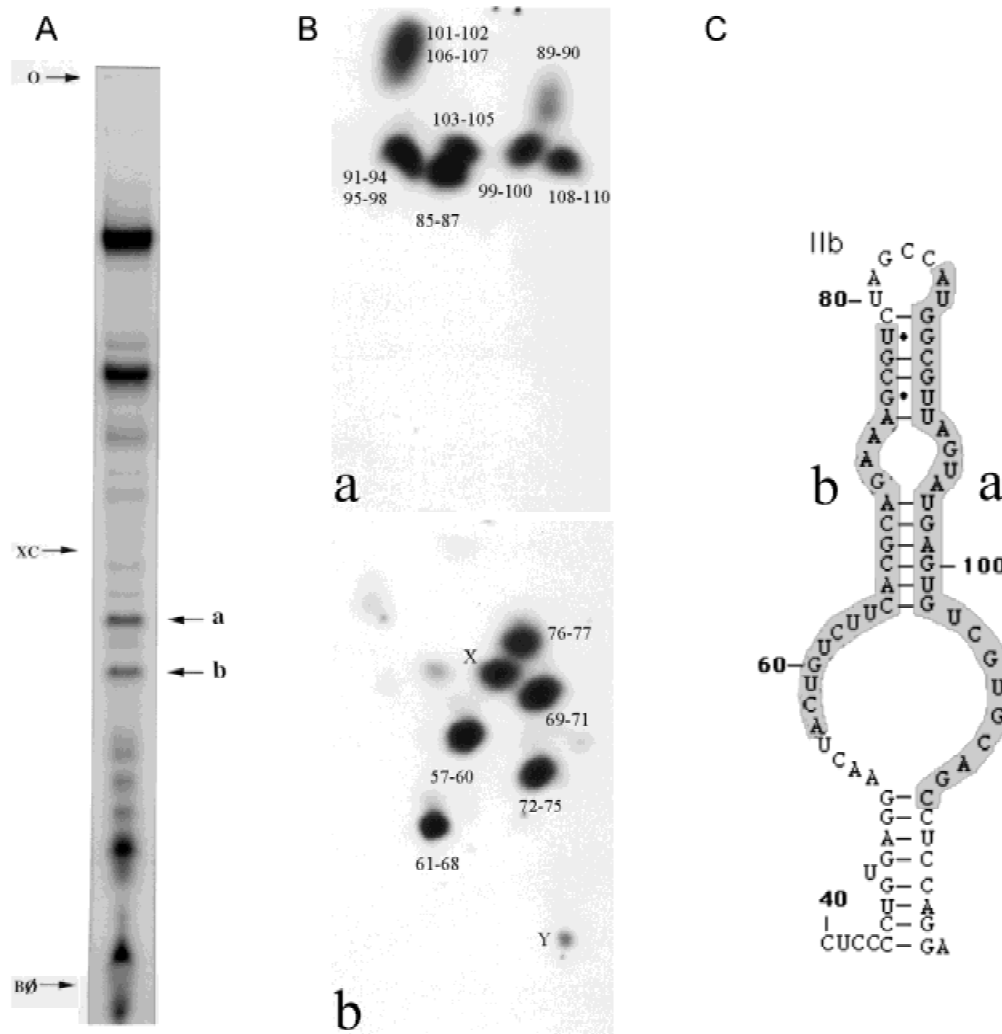
FIGURE 5. Stem-loop II protection by the 40S ribosomal subunit. **A:** Bands a and b from HCV RNA are both protected by purified 40S subunits. They were electrophoresed on a denaturing, polyacrylamide gel and then extracted. **B:** Band a (a) and band b (b) were subjected to RNA fingerprinting. The oligomers were extracted from the DEAE-cellulose and their sequence identified by further secondary analyses. Spots X and Y represent a separate sequence of similar size to sequence B which, therefore, ran the same distance in the gel as sequence b. **C:** Band a and band b are depicted on the secondary structural map of stem-loop II of the HCV IRES.

49 and 353 (Fig. 6A, green lines). However, bases 192 to 199 remain unprotected. The protected fragments are discontinuous and noncontiguous. The two largest recovered fragments lie between residues 210 and 353 and 49 and 191. The fragment spanning bases 210–353 contains the AUG initiator codon, and was only recovered one time in the course of multiple experiments. No other fragments containing this AUG triplet were observed. Several domains appear to be more frequently recovered among the protected fragments from the HCV-40S complex. These "core" domains were recovered a minimum of four separate times. Four such core domains exist: core domain Ⓐ contains residues 59–69, Ⓑ contains residues 126–141, Ⓒ contains residues 165–175, and Ⓓ contains residues 217–255. Each of these core domains contains at least 15 bases except for core domain Ⓓ, which contains 39 bases.

The region of the HCV IRES protected by the 40S ribosomal subunit is large (Fig. 6B). Core domains occur throughout the IRES and only two appear to interact: core domains Ⓒ and Ⓓ share a short region of base pairing. Core domain Ⓐ lies on the left side of stem-loop II, although the right side is often protected as well. Core domain Ⓑ includes part of the spacer region between stem-loops II and III and some of stem-loop III. Core domain Ⓒ lies in stem-loop IIIa, and core domain Ⓓ contains a large portion of stem-loop III including stem-loop IIIc. Residues 192 to 199, which comprise the apical loop of stem-loop III, were not protected in these experiments. These residues were also not protected in 48S and 80S initiation complexes (Lytle et al., 2001). As mentioned above, residues 337–355, which comprise stem-loop IV and contain the start AUG codon, were only recovered once, in one RNA fragment.
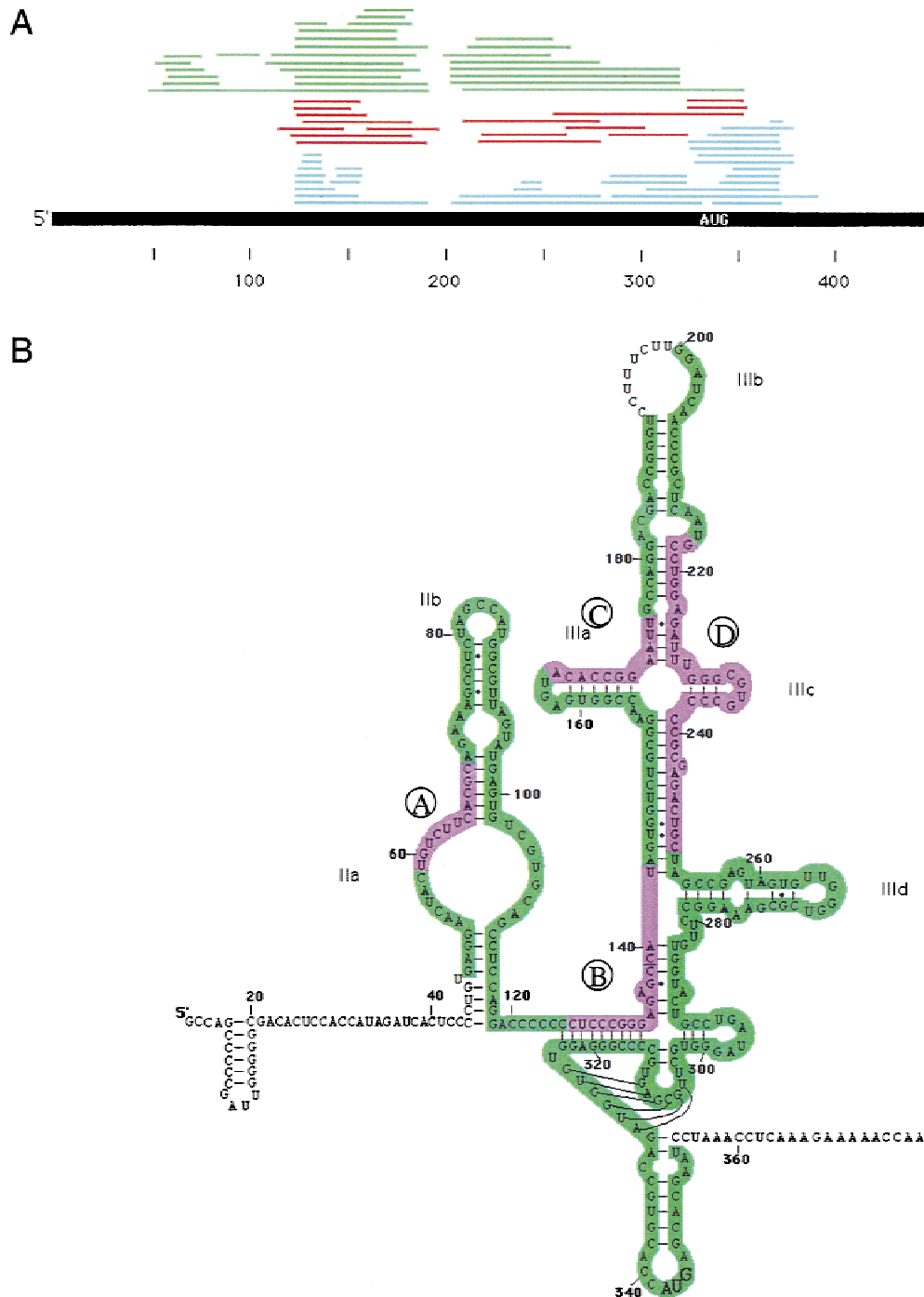
A

B

FIGURE 6. The HCV RNA fragments protected by the 40S subunit. **A:** The HCV RNA genome is depicted here as a single, thick, black line. The HCV fragments protected by the 40S subunit are shown as thin green lines. The edeine-induced 48S ribosomal protected fragments are depicted above the genome as thin red lines. The 80S ribosomal protected fragments are shown as thin blue lines. All 40S protected fragments lie within bases 49–353. The 80S protected fragments lie within bases 124–392 and the 48S protected fragments within bases 124–355. No protected fragments were found between bases 192 and 199 for the 40S ribosomal complex. **B:** The region of the HCV IRES protected from RNase by the 40S ribosomal subunit is shown in green. The core domains are shown in purple.

DISCUSSION

Our work here focuses on the ribosomal preinitiation complex formed between purified 40S ribosomal sub-

units and the HCV IRES. By analyzing the protection of the HCV IRES by 40S ribosomal subunits, we decided to study what could be the first step in the HCV translation initiation pathway. Previously, we have studied

the multicomponent 80S and 48S ribosomal complexes containing the HCV IRES (Lytle et al., 2001), which represent later stages of this process.

We found that residues 49 to 353 of the HCV IRES, which contain stem-loop II, are protected by salt-washed 40S ribosomal subunits. This protection domain contains much more 5′ sequence than any of the other ribosomal complexes we have studied (Lytle et al., 2001). Thus, as predicted by the tertiary structural probing done in this laboratory (Lyons et al., 2001), the HCV-40S complex protects stem-loop II of the HCV IRES. Like the 80S and 48S protection patterns, stem-loop III (minus the apical portion) and the pseudoknot region are protected by 40S subunits alone. However, only a single RNA fragment protected by the 40S subunit contains the coding region. All other protected RNA fragments from the HCV-40S complex end at residue 336, which corresponds to the 3′ end of the pseudoknot. Thus, the HCV-40S complex only minimally protects the start AUG codon, unlike the 80S and 48S complexes. We therefore conclude that, as the HCV-40S complex gains components to become the 48S complex, the protected domain of the HCV IRES shifts in a 3′ direction, which leaves stem-loop II unprotected at the same time that the start codon and some coding sequence become more strongly protected. We also conclude that the HCV IRES undergoes a structural transition as the 40S binary complex is converted to the 48S, and then the 80S, complexes.

Figure 6A shows the portions of the IRES protected by the three ribosomal complexes studied in this laboratory and illustrates the "rightward shift" of protection as initiation proceeds. Interestingly, between these three ribosomal complexes, almost the entire functional IRES, known to lie between residues 40 and 372, is protected. No bases 5′ to base 49 or 3′ to base 392 are protected by any of the three ribosomal complexes.

Our above suggestion that the HCV IRES undergoes a structural transition as the binary complex is converted to the 48S complex complements those of an earlier study by Spahn et al. (2001), who suggested that the 40S ribosomal subunit itself undergoes an earlier structural transition, immediately upon binding the HCV IRES. Spahn et al. (2001) propose that the HCV IRES RNA binds as a rod structure that lies on the solvent side of the 40S subunit, a finding which would help to explain the very similar protection of HCV IRES stem-loop III and the pseudoknot in the binary, 48S and 80S complexes (Figs. 6 and 7; Lytle et al., 2001). By binding to the back side of the 40S subunit, these domains of the HCV IRES could remain bound in a similar fashion throughout translation initiation, largely unaffected by addition of tRNAs, factors, or the 60S subunit.

Other than the expected increase in protection of HCV IRES sequences downstream from the initiator AUG as translation initiation progresses (Fig. 6A), the major change is that which occurs in stem-loop II protection. The cryo-electron microscope study (Spahn et al., 2001) shows this domain "reaching" over the top of the 40S subunit from the solvent side towards the E-site on the side that binds to the 60S subunit. Because stem-loop II is protected in the HCV-40S binary complex, but not in the subsequent 48S or 80S complexes, the initial interaction of the HCV IRES near the E-site must be disrupted as additional components bind to form the 48S complex. This finding leads to our hypothesis that the IRES undergoes a structural transition. Interestingly, ribosomal protein S5, which was proposed as a candidate to bind to the tertiary element we discovered in stem-loop II (Lyons et al., 2001), has been shown through antibody labeling to lie close to the E-site of the 40S subunit (Lutsch et al., 1983). Thus, stem-loop II appears to promote initial 40S subunit binding, but is not needed for the following steps.

One way in which upstream sequences could be involved in the expression of IRES-containing mRNAs involves the presence, upstream from the mRNA's normal initiator triplet, of AUG-containing sequences that encode short peptides called untranslated open reading frames (uORFs). In the case of cat-1 mRNA, translation of a uORF to yield a 48-amino-acid peptide sequence has been invoked as one regulatory step in the adaptive response of cells to amino acid limitation (Fernandez et al., 2001). The HCV IRES has three AUG-containing uORFs, of which two begin in stem-loop II. Although it remains possible that recognition of these elements could play a role in protection of stem-loop II by 40S subunits, the lack of such protection in the 48S and 80S complexes (Fig. 6; Lytle et al., 2001) suggests that these HCV uORFS, unlike their cat-1 mRNA counterpart, are not translated under these conditions.

Using our current and prior results (Lytle et al., 2001) and data from the literature, a model of the HCV translation initiation pathway has been proposed in Figure 7. Even in the presence of the ternary complex and multiple initiation factors, HCV recognition of the 40S subunit—through RNA–RNA or RNA–protein contacts—may be the primary determinant for initial association to form the binary complex between the HCV IRES and the 40S ribosomal subunit. We favor this point of view despite the likelihood that most 40S subunits contain eIF3 in lysates and cells (Hershey & Merrick, 2000). Thus, in Figure 7, the pathway in the top left, where eIF3 binds to the IRES first, may be favored over that on the top right, which involves the binary complex. However, a recent study shows that the binding affinity of the HCV IRES for the 40S subunit alone is virtually identical to its affinity for the 40S-eIF3 complex (Kieft et al., 2001). It is therefore unlikely that the HCV IRES's specificity determinants for binary complex formation, which we have identified here, are much affected by the presence or absence of eIF3.
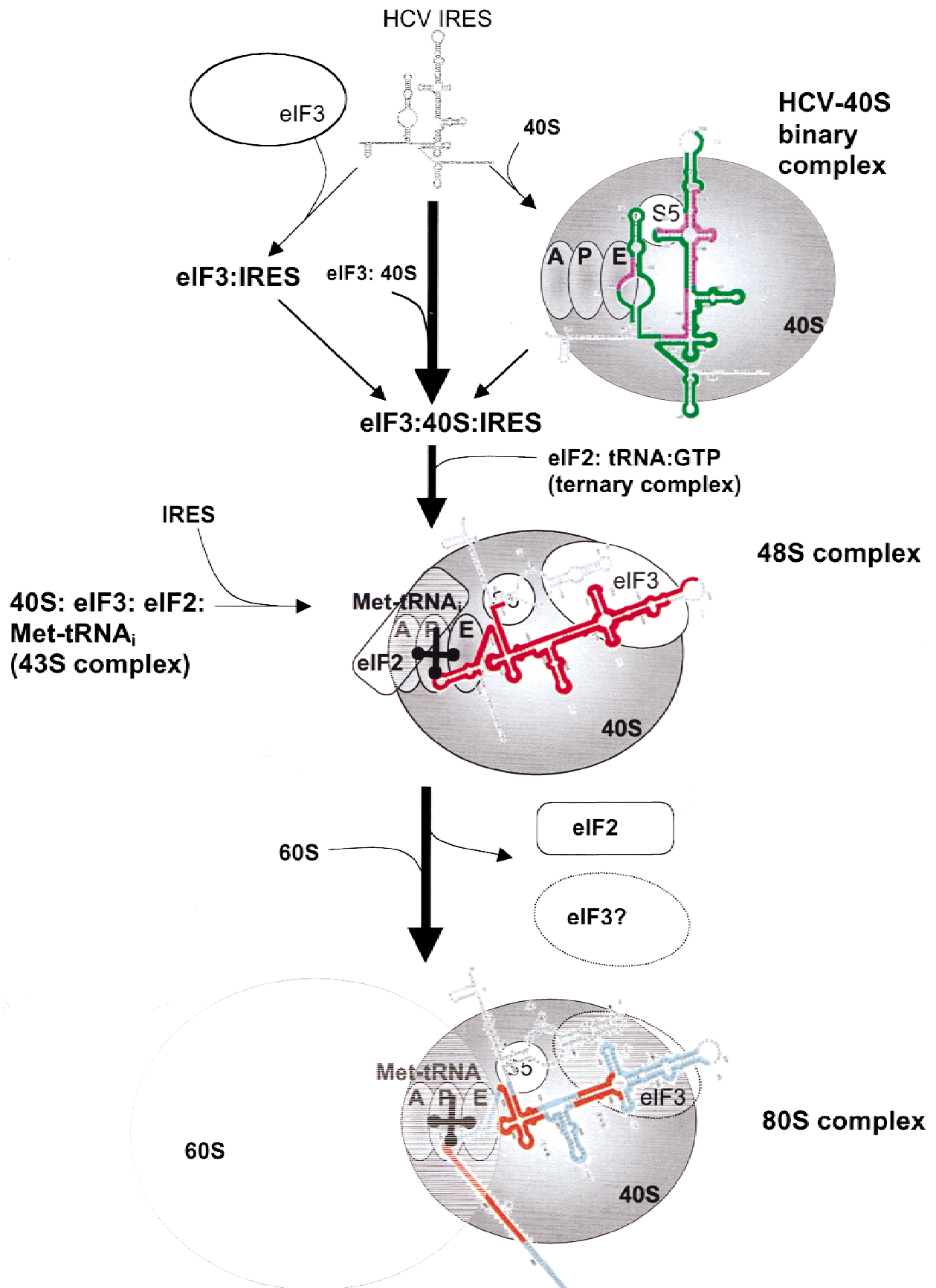
FIGURE 7. The translation initiation pathway of the HCV IRES. This model is based on previously published work (Lytle et al., 2001), work published here, and data from the literature.

Stem-loop II, stem-loop III, and the pseudoknot domain of the HCV IRES bind to purified 40S ribosomal subunits (Fig. 7, shown in green and purple), but bases beyond residue 336, including the AUG start codon, are not well protected in the HCV-40S binary complex. Protection of the HCV IRES shifts in the 48S ribosomal complex (shown in red). eIF3 most likely binds to the upper portion of stem-loop III and affords some protection (Pestova et al., 1998). Codon–anticodon base pairs probably begin to form between Met-tRNA$_i$ of the ternary complex and the start codon of the IRES. The stronger protection of the start codon and the HCV coding sequence that we observed before (Lytle et al., 2001) is presumably due to this interaction. Bases between 115 and 355 of the HCV IRES are now protected. Stem-loop II, which was involved initially in 40S subunit recognition, is no longer protected. Instead, protection of the HCV IRES shifts from stem-loop II toward stem-loops III and IV and the pseudoknot domain. Perhaps a component such as eIF3, the ternary complex, or a noncanonical factor causes the shift in IRES structure, leading to the displacement of stem-loop II from its binding site on the 40S subunit.

The 80S ribosomal complex again shifts HCV protection (Fig. 7, shown in blue with the core domains in orange). Protection shifts to cover more 3′ sequence of the HCV IRES, and 50 bases of coding sequence are now involved. As we suggested before (Lytle et al., 2001), eIF3 may remain in this HCV 80S ribosomal complex. The "core" protected regions of this complex are complementary regions in mid stem-loop III, almost the entire pseudoknot domain, and the start codon and 50 bases of coding sequence. Protection of the start codon and coding region is presumably caused by the involvement of the coding region of the mRNA in threading itself through the 80S ribosome in a manner similar to that of unstructured, eukaryotic mRNAs.

By using direct techniques to study the domains of the HCV IRES that interact with the 80S, the 48S, and the 40S ribosomal initiation complexes, we have discovered which portions of the HCV IRES are necessary at each step of HCV translation initiation. Thus far, only indirect data were available for any of these complexes. Knowledge of the domains of the HCV IRES that participate in the different stages of translation initiation should clarify our understanding of IRES function, and should also help in the development of antiviral therapies targeted to the IRES translation mechanism.

MATERIALS AND METHODS

In vitro transcription

The plasmid pN(1-4728) containing the first 4.7 kb of hepatitis C virus sequence adjacent to the phage T7 promoter was a gift from Dr. Stanley Lemon, University of Texas, Galveston.

The plasmid was cleaved by the different restriction enzymes: *Nhe*I, *Aat*II, and *Sac*II. When these templates were transcribed in vitro, three ^{32}P-labeled RNAs spanning bases 1–249, 1–402, and 1–645 were produced. The plasmid pβHb containing rabbit β globin cDNA was a gift from Dr. Karen Browning, University of Texas, Austin. This plasmid was cleaved with *Hin*dIII to produce the proper template for transcription. RNA synthesis in vitro was carried out in 20–60 μL volumes in siliconized 13 $\times$ 54 mm glass tubes. Each reaction contained 50–100 U of phage T7 RNA polymerase (Pharmacia), 1–3 μg linearized DNA template, 40 mM Tris-HCl, pH 7.5, 10 mM MgCl$_2$, 2 mM spermidine, 10 mM NaCl, 5 mM DTT, 50 μg BSA (RNase free; Sigma), 40 U/μL RNasin (Promega), 0.4 mM cold rNTPs, and 20–120 μCi [α-^{32}P]-GTP or -CTP (3,000 Ci/mmol; Perkin-Elmer). The 60-μL reactions reduced the concentration of cold ribonucleotides corresponding to radiolabeled nucleotide by fivefold to create a high specific activity. Such reactions yield RNA specific activities of 4.13 $\times$ 10^6 dpm/μg or 8.25 $\times$ 10^7 dpm/μg. To create capped β-globin transcripts, each reaction contained 50–100 U of phage T7 RNA polymerase (Pharmacia), 1–3 μg linearized DNA template, 40 mM Tris-HCl, pH 7.5, 6 mM MgCl$_2$, 2 mM spermidine, 10 mM NaCl, 10 mM DTT, 10 μg/μL BSA (RNase free-Sigma), 1 mM cap analog (Ambion), 40 U/μL RNasin (Promega), and 20–120 μCi [α-^{32}P]-GTP or -CTP (3,000 Ci/mmol; Perkin-Elmer). Such reactions yield RNA-specific activities of 4.13 $\times$ 10^6 dpm/μg or 8.25 $\times$ 10^7 dpm/μg.

Purification of 40S subunits

Salt-washed ribosomes were a gift from Dr. William Merrick, Case Western Reserve University, Cleveland. The salt-washed ribosomes were dissolved in 50 mM HEPES-KOH, pH 7.5, 2 mM MgCl$_2$, 1 mM puromycin, and 500 mM KCl at a concentration of 50 A260 U/mL (Merrick, 1979). The solution was incubated on ice for 15 min and then heated at 37 °C for 10 min. The solution was then chilled on ice. The solution was divided into six aliquots and layered on 5 mL 15–30% sucrose density gradients containing 50 mM HEPES-KOH, pH 7.5, 5 mM MgCl$_2$, 2 mM dithiothreitol, 500 mM KCl, and 0.1 mM EDTA. The six gradients were spun for 2 h at 45,000 rpm at 4 °C. The back half of the 40S peak was collected to prevent contamination by 60S subunits. The fractions were collected and centrifuged for 5.5 h at 45,000 rpm (189,378 $\times$ g average) at 4 °C. The pellet was dissolved in 500 μL of 0.25 M sucrose, 1 mM MgCl$_2$, 1 mM dithiothreitol, 10 mM KCl, and 0.2 mM EDTA to a concentration of 0.6 pmol/μL.

Ribosome binding

Ribosome-binding reactions with anisomycin-induced 80S ribosomal complexes and edeine-induced 48S ribosomal complexes were described previously (Lytle et al., 2001).

Purified 40S subunit binding and protection

40S subunit binding reactions were created to mimic Promega's standard translation protocol, which was used in the binding reactions of 80S and 48S ribosomal complexes in rabbit reticulocyte lysate (Lytle et al., 2001). Each sample

had a final reaction volume that equaled 50 μL. If necessary, 10 mM EDTA was added to control reactions at this time. One microgram of radiolabeled HCV mRNA (1–402 or 1–645) and 26.3 pmol of salt-washed 40S ribosomal subunits were added to each reaction. Each reaction contained 20 mM Tris-HCl, pH 7.5, 2.5 mM MgAc, and 100 mM KCl. The samples were incubated for 15 min at 30 °C and then immediately placed on ice. Pancreatic RNase A was added to each sample (0.4 μg/mL final concentration) followed by incubation on ice for 7.5 min. This RNase concentration was determined by titration to be the minimum amount under these conditions that would lead to complete digestion of the HCV RNA in the absence of binding to 40S subunits. In particular, experiments carried out with the complete system, but in the presence of EDTA, have been used here and before (Lytle et al., 2001) to demonstrate complete digestion of the HCV IRES sequences and the absence of any cosedimentation of RNA fragments with the peak of 40S subunits (Fig. 3). RNA fragments obtained from the complete system, lacking EDTA, have several reproducible properties. First, because they are produced by pancreatic RNase cleavage, they all have pyrimidine residues at their 3′ termini. The RNase T1 fingerprinting assays used to characterize these fragments (Fig. 5) are based on cleavage to yield oligonucleotides with G-residues at their 3′ termini. Therefore, the 5′ end of each fragment will usually yield a truncated RNase T1-specific oligonucleotide (cut at an interior pyrimidine), whereas the 3′ termini will be pyrimidines, rather than G-residues.

The second striking property of such ribosome-protected HCV IRES fragments is the reproducible pattern of heterogeneous gel bands obtained following purification of the protected RNA fragments and polyacrylamide gel electrophoresis as in Figure 4. Because the pancreatic RNase digestion is sufficiently exhaustive, we can rule out the recovery here of parts of the IRES that cosediment with the 40S subunit but are not really in contact with it. However, some parts of the IRES may be in close but not intimate contact with the 40S subunit, giving the opportunities for pancreatic RNase to cut at internal sites with a probability characteristic of each site. This would explain both the heterogeneity and the reproducibility of the patterns observed here and before (Lytle et al., 2001).

Sucrose density gradient analysis

After 7.5 min (for 40S subunits) on ice, 250 μL of gradient buffer (25 mM KCl, 10 mM NaCl, 1 mM MgCl$_2$, 10 mM Tris-HCl, pH 7.5, and 1 mM dithiothreitol) was added to each reaction and the samples were loaded onto 5-mL 15–30% sucrose gradients using the same gradient buffer. Gradient buffer similar to that described above without MgCl$_2$ and containing 10 mM EDTA was used both for dilution of samples and formation of 5-mL 15–30% sucrose gradients containing EDTA. All samples were then centrifuged for 2 h at 4 °C and 45,000 rpm (189,378 $\times$ g average). Two-drop fractions were collected as before (Legon et al., 1976) and those corresponding to the appropriate peaks were pooled. The total volume containing the 40S peaks was approximately 1 mL. Protected RNA was recovered from pooled fractions as before (Legon et al., 1976). Pooled 40S peaks were added to 1 mL of phenol containing 0.5 g urea, 10 μL of mercaptoethanol, 10 μL of 10% sodium dodecyl sulphate, and 10 μL of 200 mM EDTA at ambient temperature. The mixture was vortexed, 1 mL of chloroform was added, and, after more vortexing, the phases were separated by centrifugation. The aqueous layer was collected and ethanol precipitated.

RNA fingerprinting

This technique was carried out using the standard method (Barrell, 1971; Branch et al., 1989). Briefly, the radioactive RNA of interest, along with 10 μg of tRNA carrier, was digested with 1 mg/mL RNase T1, which cleaves after G-residues, for 40 min at 37 °C. The fragments were then analyzed on a two-dimensional system (Brownlee & Sanger, 1969), in which the first dimension is a 10% polyacrylamide gel run at pH 3.5 and in 7 M urea (which separates the RNA fragments by base composition) followed by a second dimension of ascending RNA homochromatography (which separates the RNase T1-resistant oligonucleotides on the basis of size) on 20 $\times$ 40 cm thin-layer DEAE cellulose (Machery-Nagel/Alltech). The resulting fingerprint pattern, obtained by autoradiography, is unique for each RNA sequence.

Further analysis of RNase T1-resistant oligonucleotides was carried out, following their elution from the thin layers by conventional techniques (Barrell, 1971), by treatment of aliquots with RNase T2 (which yields nucleoside 3′ monophosphates) or pancreatic RNase A (which cleaves after pyrimidines) under standard conditions first published by Barrell (1971). Products of these secondary digestions were separated by one-dimensional high-voltage electrophoresis at pH 3.5 on 3MM (RNase T2) or DEAE (RNase A) papers (Whatman) and detected by autoradiography.

REFERENCES

Allison LA, Romaniuk PJ, Bakken AH. 1991. RNA–protein interactions of stored 5S RNA with TFIIIA and ribosomal protein L5 during *Xenopus* oogenesis. *Dev Biol 144*:129–144.
Barrell BG. 1971. Fractionation and sequence analysis of radioactive nucleotides. In: Cantoni GL, Davies DR, eds. *Procedures in nucleic acid research.* New York: Harper and Row. pp 751–795.
Branch AD, Benenfeld BJ, Robertson HD. 1985. Ultraviolet light-induced crosslinking reveals a unique region of local tertiary structure in potato spindle tuber viroid and HeLa 5S RNA. *Proc Natl Acad Sci USA 82*:6590–6594.
Branch AD, Benenfeld BJ, Robertson HD. 1989. RNA fingerprinting. *Methods Enzymol 180*:130–154.
Brownlee GG, Sanger F. 1969. Chromatography of ^{32}P-labelled oligonucleotides on thin layers of DEAE-cellulose. *European J Biochem 11*:395–399.
Dever TE. 1999. Translation initiation: Adept at adapting. *Trends Biochem Sci 24*:398–403.

Fernandez J, Yaman I, Merrick WC, Koromilas A, Wek RC, Sood R, Hensold J, Hatzoglou M. 2001. Regulation of internal ribosome entry site-mediated translation by eukaryotic initiation factor-2α phosphorylation and translation of a small upstream open reading frame. *J Biol Chem 277*:2050–2058.

Fukushi S, Katayama K, Kurihara C, Ishiyama N, Hoshino FB, Ando T, Oya A. 1994. Complete 5′ noncoding region is necessary for the efficient internal initiation of hepatitis C virus RNA. *Biochem Biophys Res Commun 199*:425–432.

Fukushi S, Okada M, Kageyama T, Hoshino FB, Katayama K. 1999. Specific interaction of a 25-kilodalton cellular protein, a 40S ribosomal subunit protein, with the internal ribosome entry site of hepatitis C virus genome. *Virus Genes 19*:153–161.

Fukushi S, Okada M, Stahl J, Kageyama T, Hoshino FB, Katayama K. 2001. Ribosomal protein S5 interacts with the internal ribosomal entry site of hepatitis C virus. *J Biol Chem 276*:20824–20826.

Hershey JWB, Merrick WC. 2000. The pathway and mechanism of initiation of protein synthesis. In: Sonenberg N, Hershey JWB, Mathews MB, eds. *Translational control of gene expression*. Cold Spring Harbor, New York: Cold Spring Harbor Laboratory Press. pp 33–88.

Honda M, Beard MR, Ping L-H, Lemon SM. 1999. A phylogenetically conserved stem-loop structure at the 5′ border of the internal ribosome entry site of hepatitis C virus is required for cap-independent viral translation. *J Virol 73*:1165–1174.

Honda M, Ping L-H, Rijnbrand RCA, Amphlett E, Clarke B, Rowlands D, Lemon SM. 1996. Structural requirements for initiation of translation by internal ribosome entry within genome-length hepatitis C virus RNA. *Virology 222*:31–42.

Kieft JS, Zhou K, Jubin R, Doudna JA. 2001. Mechanism of ribosome recruitment by hepatitis C IRES RNA. *RNA 7*:194–206.

Kolupaeva VG, Pestova TV, Hellen CUT. 2000. An enzymatic footprinting analysis of the interaction of 40S ribosomal subunits with the internal ribosomal entry site of hepatitis C virus. *J Virol 74*:6242–6250.

Legon S, Robertson HD, Prensky W. 1976. The binding of ^{125}I-labelled rabbit globin messenger RNA to reticulocyte ribosomes. *J Mol Biol 106*:23–36.

Lutsch G, Bielka H, Enzmann G, Noll F. 1983. Electron microscopic investigations on the location of rat liver ribosomal proteins S3a, S5, S6, S7 and S9 by means of antibody labeling. *Biomed Biochim Acta 42*:705–723.

Lyons AJ, Lytle JR, Gomez J, Robertson HD. 2001. Hepatitis C virus internal ribosome entry site RNA contains a tertiary structural element in a functional domain of stem-loop II. *Nucleic Acids Res 29*:2535–2541.

Lytle JR, Wu L, Robertson HD. 2001. Ribosomal binding domains of the hepatitis C virus internal ribosome entry site. *J Virol 75*:7629–7636.

Merrick WC. 1979. Assays for eukaryotic protein synthesis. *Methods Enzymol 60*:108–123.

Odreman-Macchioli F, Baralle FE, Buratti E. 2001. Mutational analysis of the different bulge regions of hepatitis C virus domain II and their influence on internal ribosome entry site translational ability. *J Biol Chem 276*:41648–41655.

Odreman-Macchioli FE, Tisminetzky SG, Zotti M, Baralle FE, Buratti E. 2000. Influence of correct secondary and tertiary RNA folding on the binding of cellular factors to the HCV IRES. *Nucleic Acids Res 28*:875–885.

Pestova TV, Kolupaeva VG, Lomakin IB, Pilipenko EV, Shatsky IN, Agol VI, Hellen CUT. 2001. Molecular mechanisms of translation initiation in eukaryotes. *Proc Natl Acad Sci USA 98*:7029–7036.

Pestova TV, Shatsky IN, Fletcher SP, Jackson RJ, Hellen CUT. 1998. A prokaryotic-like mode of cytoplasmic eukaryotic ribosome binding to the initiation codon during internal translation initiation of hepatitis C and classical swine fever virus RNAs. *Genes & Dev 12*:67–83.

Reynolds JE, Kaminski A, Carroll AR, Clarke BE, Rowlands DJ, Jackson RJ. 1996. Internal initiation of translation of hepatitis C virus RNA: The ribosome entry site is at the authentic initiation codon. *RNA 2*:867–878.

Rijnbrand R, Bredenbeek P, van der Straaten T, Whetter L, Inchauspe G, Lemon S, Spaan W. 1995. Almost the entire 5′ non-translated region of hepatitis C virus is required for cap-independent translation. *FEBS Lett 365*:115–119.

Romaniuk PJ. 1989. Characterization of the equilibrium binding of *Xenopus* transcription factor IIIA to the 5 S RNA gene. *Biochemistry 28*:1388–1395.

Spahn CMT, Kieft JS, Grassucci RA, Penczek PA, Zhou K, Doudna JA, Frank J. 2001. Hepatitis C virus IRES RNA-induced changes in the conformation of the 40S ribosomal subunit. *Science 291*:1959–1962.

Wimberly B, Varani G, Tinoco IJ Jr. 1993. The conformation of loop E of eukaryotic 5S ribosomal RNA. *Biochemistry 32*:1078–1087.